ELSEVIER

Journal of Alloys and Compounds 387 (2005) 47–51

Journal of ALLOYS AND COMPOUNDS

www.elsevier.com/locate/jallcom

Determination of the crystal structure of $Mg(AlH_4)_2$ by combined X-ray and neutron diffraction

A. Fossdal[a,*], H.W. Brinks[a], M. Fichtner[b], B.C. Hauback[a]

[a] *Department of Physics, Institute for Energy Technology, P.O. Box 40, NO-2027 Kjeller, Norway*
[b] *Karlsruhe Research Center, Institute of Nanotechnology, P.O. Box 3640, D-76021 Karlsruhe, Germany*

Received 2 June 2004; accepted 17 June 2004

Abstract

The structure of magnesium alanate, $Mg(AlH_4)_2$, has been examined in detail by combined powder synchrotron X-ray and neutron diffraction. The space group is confirmed to be $P\bar{3}m1$ with unit cell dimensions of a = 5.2084(3) Å and c = 5.8392(5) Å at 8 K, a = 5.20309(12) Å and c = 5.8400(2) Å at 111 K and a = 5.1949(2) Å and c = 5.8537(2) Å at 295 K. The structure consists of isolated and slightly distorted AlH_4^- tetrahedra that are connected via six-coordinated Mg atoms in a distorted octahedral geometry, resulting in a sheet-like structure along the crystallographic c-axis. The distortion of the AlH_4^- tetrahedra decreases with increasing temperature, whereas, the opposite is the case for the MgH_6 octahedra. The Al–H distances are 1.606(10)–1.634(4) Å, 1.602(10)–1.682(3) Å and 1.561(12)–1.672(4) Å at 8, 111 and 295 K, respectively.

Keywords: Hydrogen storage materials; Crystal structure; Neutron diffraction; Synchrotron radiation; Alanates

1. Introduction

The alkali alanates, such as $NaAlH_4$ and $LiAlH_4$, have attracted considerable attention over the last few years due to their potential use as lightweight materials for reversible hydrogen storage [1–8]. Magnesium alanate, $Mg(AlH_4)_2$, an alkaline earth alanate, is another potential hydrogen storage candidate with a hydrogen content of 9.3 wt.%. This compound decomposes in a two-step reaction:

$$Mg(AlH_4)_2 \rightarrow MgH_2 + 2Al + 3H_2 \quad (7.0\,\text{wt.\% released hydrogen}) \quad (1)$$

$$MgH_2 + 2Al \rightarrow x\alpha + y\beta + H_2 \quad (2.3\,\text{wt.\% released hydrogen}) \quad (2)$$

where α and β in reaction (2) are Al–Mg solid solutions. Reaction (1) has been found to occur at temperatures of 135–163 °C [9–11]. The second reaction step has been reported at 270–310 °C [10,12].

The synthesis of magnesium alanate, with the purpose of use as a reducing agent in organic chemistry, was described in the literature already in the 1950s [9,13]. However, the described methods were not able to deliver gram amounts of a pure product, and an improved synthesis procedure was published recently [14]. Several reports exist on the crystal structure of solvent adducts of $Mg(AlH_4)_2$ [14–16], however, the crystal structure of the pure compound was only recently investigated by Fichtner et al. [17]. In this study, FTIR spectroscopy and knowledge of the structure of solvent adducts were used to develop a starting structure estimation. The energetically most favorable structure was suggested from density functional theory (DFT) calculations and the positions of the metal atoms, Mg and Al, were confirmed by powder X-ray diffraction.

In the present study, the complete crystal structure of magnesium alanate has been investigated by combined powder synchrotron X-ray diffraction and high-resolution powder neutron diffraction at 111 and 295 K. In addition, results from refinement of high-resolution powder neutron diffraction data

* Corresponding author. Tel.: +47-63-80-62-73; fax: +47-63-81-09-20.
E-mail address: anita.fossdal@ife.no (A. Fossdal).

0925-8388/$ – see front matter © 2004 Elsevier B.V. All rights reserved.
doi:10.1016/j.jallcom.2004.06.050

at 8 K are presented. For structural studies by neutron diffraction, use of the deuterated magnesium alanate, $Mg(AlD_4)_2$, would have been preferable. This compound has, however, not yet been synthesized, hence, the current investigations were performed on the hydride, $Mg(AlH_4)_2$.

2. Experimental

$Mg(AlH_4)_2$ was synthesized via a metathesis reaction of $NaAlH_4$ and $MgCl_2$ in diethyl ether, with subsequent purification and solvent removal. The procedure is described in detail elsewhere [14]. Due to the preparation route, NaCl is present as a secondary phase in the resulting white powder. NaCl was included in the Rietveld refinements (space group, $Fm\bar{3}m$, a = 5.6394(4) Å at 295 K), and the content of NaCl was found to be approximately 5 wt.%.

Powder X-ray diffraction (PXD) data at 111 and 295 K were collected at the Swiss–Norwegian beam line (station BM01B) at the European Synchrotron Radiation Facility (ESRF) in Grenoble, France. The sample was contained in a rotating 0.5 mm boron–silica–glass capillary. Data was collected between 2θ = 4.0 and 34.0° in steps of $\Delta(2\theta)$ = 0.006°. The wavelength was 0.49956 Å, obtained from a channel-cut Si (111) monochromator. A temperature of 111 K was obtained with a Oxford Cryostream series 600 cold nitrogen blower.

Powder neutron diffraction (PND) data at 8, 111 and 295 K were collected from 10 to 130° in 2θ with the PUS instrument at the JEEP II reactor at Kjeller (Norway) [18]. Monochromatized neutrons with λ = 1.5546 Å (1.5554 Å for the 8 K measurements) were obtained from a Ge (511) focussing monochromator. The detector unit consists of two banks of seven position-sensitive ^{3}He detectors, each covering 20° in 2θ (binned in steps of 0.05°). The sample was placed in a cylindrical V sample holder with 8 mm diameter. Data at 295 K were collected during sample rotation. Temperatures of 8 and 111 K were obtained by means of a Displex cooling system. The regions 76.30–77.55° and 115.60–117.70° were excluded in the analysis of the 8 and 111 K PND data due to additional scattering from the cooling system. Due to incoherent scattering from hydrogen, the PND measurements were performed in high-intensity mode and with long measurement times (2 days at 295 K and 4 days at 8 and 111 K) to maximize the signal-to-noise ratio. The long measurement times resulted in discontinuities in the diffractogram at the changeover point between the different detector banks. For that reason, the regions 69.50–70.50°, 89.80–90.40° and 109.60–110.30° were excluded from further analysis for the PND data.

Rietveld refinements were carried out with the program Fullprof (Version 2.50) [19]. The neutron scattering lengths b_{Mg} = 5.38 pm, b_{Al} = 3.45 pm and b_H = −3.74 pm and X-ray form factor coefficients were taken from the Fullprof library. The PND and PXD data were given the weights 0.75 and 0.25, respectively, in the refinements. Pseudo-Voigt profile parameters were used and linear interpolation between manually selected points (48 for PND at 8 K, 61 for PND at 111 K, 33 for PND at 295 K and 70 for PXD at 111 and 295 K) were used for background modelling. In total, 29 parameters were varied in the final refinement for the combined PND and PXD 295 K data. For $Mg(AlH_4)_2$: one scale factor, nine structural parameters and eleven profile parameters, for NaCl: one scale factor, one structural parameter and four profile parameters, and in addition, two zero points. In the refinement of the 111 K data, one additional profile parameter was varied for $Mg(AlH_4)_2$. In the 8 K refinement, 18 parameters were varied. $Mg(AlH_4)_2$: one scale factor, ten structural parameters and four profile parameters. NaCl: one scale factor and one structural parameter. In addition, one zero point was varied.

3. Results and discussion

The atomic coordinates published by Fichtner et al. [17] were used as starting parameters in the Rietveld refinements. Unit cell parameters for $Mg(AlH_4)_2$ and reliability factors for the refinements at 8 K (PND), 111 and 295 K (combined PND and PXD) are given in Table 1. Interestingly, the crystallographic a-axis contracts somewhat upon heating from 8 to 295 K, $\Delta a/a$ = −0.26%, whereas the c-axis shows a small expansion, $\Delta c/c$ = 0.25%. Table 2 lists the calculated atomic coordinates and displacement parameters obtained from the Rietveld refinements. The displacement factors for hydrogen are high, even at 8 K, possibly due to the low decomposition temperature of $Mg(AlH_4)_2$. High thermal displacement factors have also been observed for D in $NaAlD_4$ [20] and $LiAlD_4$ [21]. The fits from the combined PND and PXD Rietveld refinements at 295 K are shown in Fig. 1. Note especially in Fig. 1a that although the hydride, rather than the deuteride, was used in this study, the signal-to-noise ratio is surprisingly good. The space group of $Mg(AlH_4)_2$ is confirmed to be $P\bar{3}m1$.

The crystal structure of $Mg(AlH_4)_2$ is illustrated in Fig. 2. The structure can be viewed as consisting of isolated, slightly distorted AlH_4^- tetrahedra. Each Mg atom is six-coordinated

Table 1
Refined unit cell parameters and reliability factors for $Mg(AlH_4)_2$, space group $P\bar{3}m1$, Z = 4, at 8, 111 and 295 K

	8 K	111 K	295 K
a (Å)	5.2084(3)	5.20309(12)	5.1949(2)
c (Å)	5.8392(5)	5.8400(2)	5.8537(2)
R_{wp} (%)			
PXD		4.79	5.70
PND	0.85	0.93	1.09
R_p (%)			
PXD		3.63	4.37
PND	0.67	0.71	0.86
χ^2	1.11	1.72	1.53

Estimated standard deviations are given in parentheses.

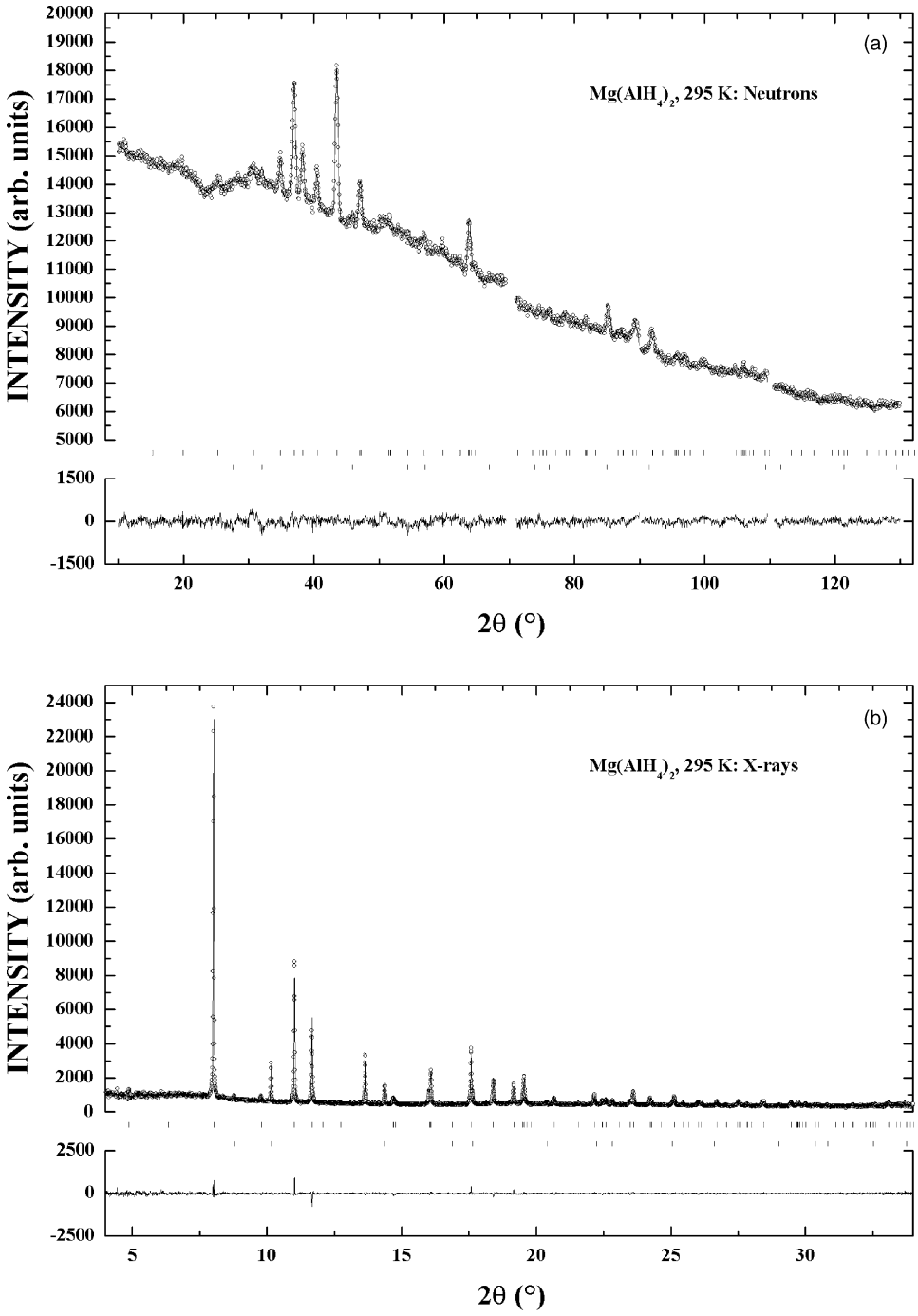

Fig. 1. (a) PND and (b) PXD patterns for $Mg(AlH_4)_2$ at 295 K showing observed (circles), calculated (upper line) and difference (bottom line) plots. The positions of the Bragg reflections are shown for $Mg(AlH_4)_2$ (upper) and NaCl (lower).

with respect to H, sharing one corner with each of six different AlH_4^- tetrahedra to form a distorted MgH_6 octahedron. The bridging hydrogen atoms are located on the H2 site, whereas, the hydrogen atoms in the H1 position are terminally bonded in the crystallographic *c*-direction. This atomic arrangement thus results in a sheet-like structure along the *c*-axis and confirms the crystal structure suggested by Fichtner et al. [17]. The sheets in the **ab** plane are interconnected by van der Waals forces rather than atomic bonds. Magnesium alanate can be described as having a CdI_2 layer structure, with AlH_4^- tetrahedra in hexagonal close packing. Mg atoms then occupy in total half of the octahedral sites, layers of fully occupied octahedral sites alternating with layers in which all the octahedral sites are empty.

Selected inter-atomic distances and bond angles are shown in Table 3. The shortest H–H distance is found between H2 atoms within the AlH_4^- tetrahedra and is directed along the *a*-axis. This distance decreases from 2.597 Å at 8 K to 2.476 Å

Table 2
Atomic coordinates, isotropic displacement factors (Å^2) for $Mg(AlH_4)_2$ at 8, 111 and 295 K

T (K)	Atom	x	y	z	B
8	Mg (1*a*)	0	0	0	0.53(8)
	Al (2*d*)	1/3	2/3	0.6991(12)	0.16(8)
	H1 (2*d*)	1/3	2/3	0.4242(12)	2.89(15)
	H2 (6*i*)	0.1671(8)	−0.1671(8)	0.8105(11)	2.47(7)
111	Mg (1*a*)	0	0	0	0.87(8)
	Al (2*d*)	1/3	2/3	0.7032(4)	0.41(4)
	H1 (2*d*)	1/3	2/3	0.429(2)	3.84(9)
	H2 (6*i*)	0.1604(11)	−0.1604(11)	0.8114(15)	3.84(9)
295	Mg (1*a*)	0	0	0	1.99(12)
	Al (2*d*)	1/3	2/3	0.7057(5)	1.17(7)
	H1 (2*d*)	1/3	2/3	0.439(2)	4.66(15)
	H2 (6*i*)	0.1589(14)	−0.1589(14)	0.804(2)	4.66(15)

Estimated standard deviations are given in parentheses.

at 295 K upon heating, a change of −4.7%. For comparison, the D–D distance found in AlD_4^- tetrahedra at 8 K in $NaAlD_4$ is 2.620 Å [20], remaining constant within the uncertainties when the compound is heated to 295 K. The Al–H1 distance (1.561 Å at 295 K) in $Mg(AlH_4)_2$ is found to be significantly longer than the 1.46 Å found in the study by Fichtner et al. [17], however, it is substantially shorter than comparable distances found in other alanates with Al in tetrahedral coordination. In $LiAlD_4$, the Al–D distances

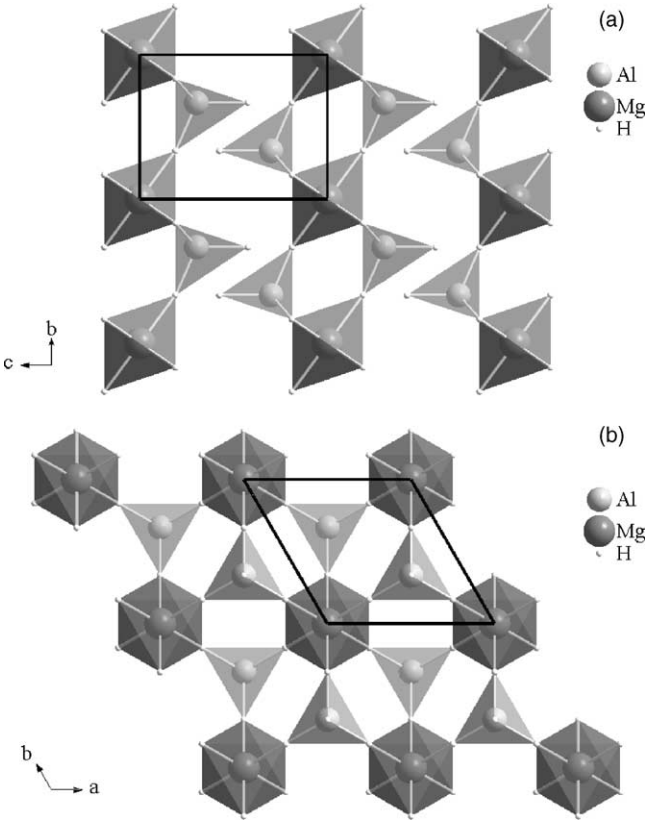

Fig. 2. Crystal structure of $Mg(AlH_4)_2$, showing six-coordinated Mg and four-coordinated Al. Views along (a) *a*-axis and (b) *c*-axis.

Table 3
Selected inter-atomic distances (Å) and angles (°) in the crystal structure of $Mg(AlH_4)_2$ at 8, 111 and 295 K

Atoms	8 K	111 K	295 K
Mg–H2	1.870(6)	1.817(8)	1.833(7)
Mg–Al	3.482(4)	3.468(1)	3.459(1)
Al–Al	3.802(6)	3.828(2)	3.846(3)
	4.624(8)	4.587(2)	4.568(3)
Al–H1	1.606(10)	1.602(10)	1.561(12)
Al–H2	1.634(4)	1.682(3)	1.672(4)
H1–H1	3.135(3)	3.117(4)	3.083(4)
H2–H1	2.709(8)	2.724(11)	2.651(13)
	2.943(5)	2.956(7)	2.962(9)
H2–H2	2.597(5)	2.504(7)	2.476(8)
	2.611(5)	2.635(11)	2.704(15)
	2.678(8)	2.699(7)	2.718(8)
H2–Mg–H2	88.55(13)	87.1(2)	85.0(2)
	91.45(13)	92.9(2)	95.0(2)
	180.0(2)	180.0(2)	180.0(3)
H1–Al–H2	113.5(2)	112.5(3)	110.1(3)
H2–Al–H2	105.24(13)	106.8(2)	108.79(15)

Estimated standard deviations are given in parentheses.

range between 1.603 and 1.633 Å [21], whereas in $NaAlD_4$, the Al–D distance is 1.626 Å at 295 K [20]. The three Al–H2 distances in $Mg(AlH_4)_2$ at 295 K are 1.672 Å, giving an average Al–H distance of 1.644 Å. The average value is very close to those found in $NaAlD_4$ and $LiAlD_4$ [20,21]. The angular distortion decreases in the AlH_4^- tetrahedra upon heating from 8 to 295 K, whereas the opposite is the case for the MgH_6 octahedra. A second-order polynomial was fitted to the changes in the H1–Al–H2 and H2–Al–H2 angles with temperature and by extrapolation of this fit both angles are expected to reach the ideal tetrahedral angle of 109.5° at 390 ± 3 K. The AlH_4^- tetrahedra will, however, not be completely regular at this temperature, as the difference between the Al–H1 and Al–H2 distances becomes larger with increasing temperature.

The unusual contraction of the *a*-axis with increasing temperature could be explained in terms of the observed changes in distortion of the polyhedra. As the angles in the AlH_4^- tetrahedra approach the ideal tetrahedral angle upon temperature increase, the distance (directed along the *a*-axis) between the bridging H2 atoms decreases. The change in H2–H2 distance between 8 and 295 K (−0.121 Å) is however much larger than the corresponding change in *a* (−0.0135 Å). The reduction of the size of the projection of the AlH_4^- tetrahedra into the **ab** plane is, therefore, partly counterbalanced by the increased distortion of the MgH_6 octahedra with increasing temperature.

Acknowledgements

The assistance by the project team at the Swiss–Norwegian Beam Line, ESRF, is gratefully acknowledged.

References

[1] B. Bogdanovic, M. Schwickardi, J. Alloy Compd. 253–254 (1997) 1.
[2] A. Zaluska, L. Zaluski, J.O. Ström-Olsen, J. Alloy Compd. 298 (2000) 125.
[3] B. Bogdanovic, M. Schwickardi, Appl. Phys. A 72 (2001) 221.
[4] C.M. Jensen, K.J. Gross, Appl. Phys. A 72 (2001) 213.
[5] J. Chen, N. Kuriyama, Q. Xu, H.T. Takeshita, T. Sakai, J. Phys. Chem. B 105 (2001) 11214.
[6] V.P. Balema, J.W. Wiench, K.W. Dennis, M. Pruski, V.K. Pecharsky, J. Alloy Compd. 329 (2001) 108.
[7] H.W. Brinks, B.C. Hauback, P. Norby, H. Fjellvåg, J. Alloy Compd. 351 (2003) 222.
[8] D. Blanchard, H.W. Brinks, B.C. Hauback, P. Norby, Mater. Sci. Eng. B 108 (2004) 54.
[9] E. Wiberg, R. Bauer, Z. Naturforsch. 7b (1952) 131.
[10] T.N. Dymova, V.N. Konoplev, A.S. Sizareva, D.P. Aleksandrov, Russ. J. Coord. Chem. 25 (1999) 312.
[11] M. Fichtner, O. Fuhr, O. Kircher, J. Alloy Compd. 356–357 (2003) 418.
[12] M. Fichtner, J. Engel, O. Kircher, O. Rubner, Mater. Sci. Eng. B 108 (2004) 42.
[13] E. Wiberg, R. Bauer, Z. Naturforsch. 5b (1950) 397.
[14] M. Fichtner, O. Fuhr, J. Alloy Compd. 345 (2002) 286.
[15] E.C. Ashby, R.D. Schwartz, B.D. James, Inorg. Chem. 9 (1970) 325.
[16] H. Noeth, M. Schmidt, A. Treitl, Chem. Ber. 128 (1995) 999.
[17] M. Fichtner, J. Engel, O. Fuhr, A. Glöss, O. Rubner, R. Ahlrichs, Inorg. Chem. 42 (2003) 7060.
[18] B.C. Hauback, H. Fjellvåg, O. Steinsvoll, K. Johansson, O.T. Buset, J. Jørgensen, J. Neutron Res. 8 (2000) 215.
[19] J. Rodríguez-Carvajal, Phys. B 192 (1993) 55.
[20] B.C. Hauback, H.W. Brinks, C.M. Jensen, K. Murphy, A.J. Maeland, J. Alloy Compd. 358 (2003) 142.
[21] B.C. Hauback, H.W. Brinks, H. Fjellvåg, J. Alloy Compd. 346 (2002) 184.